IEEE Access
Multidisciplinary | Rapid Review | Open Access Journal

Received 2 September 2023, accepted 30 September 2023, date of publication 4 October 2023, date of current version 11 October 2023.

Digital Object Identifier 10.1109/ACCESS.2023.3322102

RESEARCH ARTICLE

Most-Correlated Distribution-Based Load Balancing Scheme in Hybrid LiFi/WiGig Network

MOHAMMED FARRAG[1,2], (Member, IEEE), AND HANY S. HUSSEIN[1,3], (Senior Member, IEEE)

[1]Electrical Engineering Department, King Khalid University (KKU), Abha 62529, Saudi Arabia
[2]Electrical Engineering Department, Assiut University, Assiut 71515, Egypt
[3]Electrical Engineering Department, Aswan University, Aswan 81528, Egypt

Corresponding author: Mohammed Farrag (mohammed.farrag@eng.au.edu.eg)

This work was supported by the Deanship of Scientific Research at King Khalid University through the Small Group Project under Grant RGP.1/86/44.

ABSTRACT Recently, a hybrid network that combines radio frequency Wireless Gigabit Alliance (WiGig) networks with light fidelity (LiFi) networks has been proposed as the foundation for a high-speed wireless communication solution. A LiFi access point provides the service through the limited coverage area, LiFi attocell. Hence, LiFi networks could efficiently apply the frequency reuse concept to enhance spatial-spectral efficiency. Unfortunately, when the number of user equipment (UE) increases, new obstacles are added to those that the LiFi networks already face, such as light path obstruction, poorly aligned connections, and handover, in addition to uplink and mobility issues. To solve these issues and raise network quality of service (QoS), the hybrid LiFi/RF network has been suggested. In such networks, simultaneously and in a totally different frequency range, WiGig access points could provide tremendous data rates (gigabits per second) using the massive bandwidth of the Millimeter-Wave (mm-Wave) spectrum. Nevertheless, such hybrid networks need an effective load balancing (LB) strategy to assign the best access point (AP) and distribute enough resources for each UE depending on the location distributions of UEs (the channel between UEs and APs). The traditional LB approaches, however, use complex iterative computing procedures for each new distribution of UEs. Therefore, the Most-Correlated Distribution (MCD) Based Load Balancing Scheme is suggested in this work. The suggested method is clever enough to exploit the history of all prior load-balancing outcomes, recorded in a Distributions-Decisions Record (DDR), in order to identify appropriate allocations for the new UEs distribution, rather than going into repeated intensive complex calculations. The DDR is a list of the most common users' distributions and the corresponding best AP allocation decisions which are calculated via the Consecutive Assign WiGig First SOA (CAWFS) LB Algorithm. The DDR record is created once, and off-line via the center processing unit (CPU). Each row in the DDR is composed of the supposed distribution and the corresponding decisions. Given the new mobile user distribution, the subset of the DDR records, that contains the most correlated distributions, is constructed. The current decisions are chosen depending on the previous decisions in the selected subset via the majority voting technique. In comparison to previous load-balancing algorithms, the proposed approach intends to provide equivalent attainable data rates and outage probability performances at lower complexity.

INDEX TERMS LiFi communications, WiGig network, hybrid network, load balancing.

I. INTRODUCTION

Mobile communications networks are currently operating at their maximum capacity due to the radio frequency (RF) spectrum's limited availability and the rising number of mobile devices with multimedia content and data-demanding applications. A suggestion for a potential solution to the spectrum shortage issue is the promising Light fidelity (LiFi) technology, which operates in the 300 THz vacant and free-licensed optical region [1], [2], [3], [4]. LiFi

The associate editor coordinating the review of this manuscript and approving it for publication was Yougan Chen.

access points (APs) support communication within a few square meters of coverage area called LiFi attocells. The limited area of the attocells protects neighbouring LiFi users from interfering with nearby LiFi APs, which encourages frequency reuse and results in excellent spatial-spectral efficiency (SE) [5]. On the other side, the LiFi networks have challenges as the number of mobile device users increases, in addition to issues with mobility and uplink communication. In [6], the issues related to the theory and practice of LiFi networks for practical purposes are presented. One of these issues is user mobility and its challenges such as user light path blockage, imperfectly aligned links, and handover. Using visible light in the uplink may cause distractions to the mobile user. Due to interference between uplink and downlink, simultaneous communication couldn't be established [7]. The hybrid LiFi/RF network has been proposed in [8], [9], and [10] as a way to address these problems and improve the quality of service (QoS).

At the same time, WiGig technology offers a promising RF communication architecture that uses a new WiFi protocol with extremely high Millimetre-Wave (mmWave) transmission capacity to address the issue of spectrum scarcity [11]. WiGig has a beam steering mechanism that allows for user tracking. WiGig is, therefore, appropriate for both fixed and mobile users. On the other side, the inter-beam interference (IBI) is raised due to a rise in side-lobe levels with an increase in the number of serviced customers above a particular threshold [12], [13]. As a result, it is advised only to support a limited number of users to optimize the SE [14].

The LiFi and WiGig technologies work in totally different frequency ranges, so their applications are protected from interference, which triggers the formation of a hybrid system that integrates both LiFi and WiGig technologies [6], [15], [16], [17]. WiGig AP provides a data rate of 7 Gb/s, and simultaneously, a single light emitting diode (LED) achieves a data rate above 3 Gb/s [9], [10]. Hence, the total performance of the hybrid LiFi/WiGig network is better than that of a separate LiFi or WiGig system [17]. Moreover, the need for RF and LiFi integration networks will also be necessary next 6G network to support their use cases [18] such like eMBB (Enhanced Mobile Broadband): eMBB is one of the primary use cases of 6G, which focuses on improving the speed, capacity, and coverage of mobile broadband networks. This can be achieved by enabling the integration between Mm-Waves and LiFi, raising the need for a robust load-balancing scheme.

Each user in the hybrid network should only have access to a single AP, a LiFi, or a WiGig AP. To ensure high user throughput, fairness, and stability, a load balancing (LB) scheme is required. The access point assignment (APA) and resource allocation operations are the two fundamental components of the LB scheme (RA) [19].

For hybrid RF/Visible light communication (VLC) networks, joint load balancing (LB) and power allocation (PA) systems were suggested. To increase the total system capacity and improve system fairness, an iterative approach has been developed in [20] and [21]. In [22], an APA framework using the multicriteria decision-making (MCDM) approach for users in a hybrid LiFi/WiFi network was proposed. The optimization-based scheme (OBS), the joint and separate optimization algorithms (JOA and SOA), and the fuzzy logic-based scheme (FBS) [23] are examples of the LB schemes that are the subject of the comparative analysis in [24]. The simulation study demonstrates that JOA performs much better than SOA regarding user data rate and approaches the global optimum. Yet, SOA has considerably lower computational complexity than JOA.

Authors in [17] describe the development of two modified SOA algorithms to be applied in a hybrid network based on fusing LiFi and WiGig technologies: the Assign WiGig First SOA (AWFS) algorithm and the Consecutive Assign WiGig First SOA (CAWFS) algorithm. In the modified algorithms, only N_{max} users with the lowest LiFi data rate are chosen to be allocated to the WiGig AP, and all other users are assigned to the LiFi APs. According to the simulation results, the two suggested approaches in [17] outperformed the SOA strategy regarding feasible data rates and outage probability.

In this work, the Most-Correlated Distribution (MCD) Based Load Balancing Scheme is proposed. The proposed MCD algorithm aims to offer comparable achievable data rate and outage probability performances, with less computational complexity, compared to other LB algorithms. The main idea of the proposed MCD algorithm is not to repeat the APA optimization calculations for each users' distributions. Instead, the MCD algorithm has enough intelligence to utilize the history of all possible mobile users' distributions and their corresponding APA decisions, recorded in a Distributions-Decisions Record (DDR), to calculate the most suitable decisions for the new mobile users' distribution. Without loss of generality, the CAWFS LB Algorithm is used to determine the DDR, which is a list of the best APA decisions for the most prevalent user distributions. The DDR record is produced just once and off-line by the CPU. Each row in the DDR is made up of the assumed distribution and the related APA decisions. According to the new mobile user distribution, the subset of the DDR records with the highest correlations is constructed. Using the majority voting method, the current decisions are determined based on the prior decisions made in the specified subset. The proposed MCD introduces a novel, simple method (the lookup table approach) that can be implemented based on any co-existing load-balancing scheme to reduce its overall computational complexity.

The rest of the article is arranged as follows: Section II presents the LiFi and WiGig channel models, the hybrid system model, and a review of the SOA and CAWFS algorithms. Part III offers an in-depth explanation of the proposed MCD load balancing algorithm. Section IV provides a simulation and discussion of the throughput analysis and performance evaluation. Lastly, Section V concludes the paper.

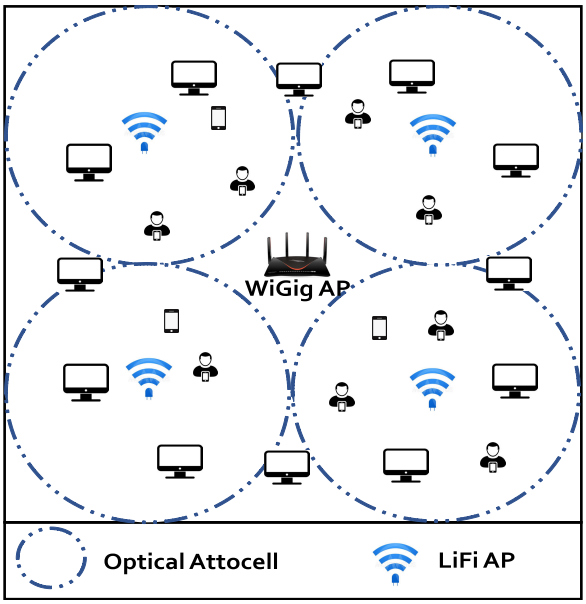

FIGURE 1. System model.

II. SYSTEM MODEL, SOA AND CAWFS ALGORITHMS

A. SYSTEM MODEL

The suggested system is depicted in Fig. 1 as including one WiGig AP and several N_{LF} LiFi APs spread across the ceiling of the coverage area. $\mathcal{U} = \{\mu_i\}_{i=1}^{N_\mu}$, a collection of N_μ users, are distributed randomly throughout the room. The system under consideration has a central unit (CU) linked to each AP, utilizing error-free connectivity. In the LiFi sub-network, the AP, which is made up of several light-emitting diodes (LEDs), communicates with the mobile receivers using photodetectors (PDs) that are perpendicular to each other and produce equal irradiance and incidence angles. The LiFi system may provide outstanding spatial efficiency (SE) since it utilizes spectrum reuse across all LiFi APs [25]. Inter-carrier interference (ICI), which can reduce the user data rate, may occur when users move in the overlapped space between adjacent cells [8], [26]. Using a WiGig AP to boost system throughput can overcome this difficulty. Each mobile user is assigned to a LiFi or a WiGig AP for downlink communication. The network load balancing (LB) system is required to handle the responsibilities of access point assignment (APA) and time slot resource allocation (RA).

In the dynamic indoor situation, the APA and RA processes should be updated each a quasi-static state T_n, where n is the sequence number of the states [26]. In the supposed system, the LiFi and WiGig APs are given as $\mathcal{C} = \{c | c \in [0, N_{LF}], c \in \mathbb{Z}\}$, where $(c = 0) \in \mathcal{C}_\mathcal{R}$ indicates to the WiGig AP and $\mathcal{C}_l = \{c\}_1^{N_{LF}}$ are the LiFi APs, and $\mathbb{Z}$ is the integer numbers set.

B. THE LIFI CHANNEL MODEL

Line of sight (LoS) and reflection constitute the two separate components of the gain of the optical channel in indoor communication conditions. The LoS component is shown from [27] as follows:

$$H_{\mu,\alpha} = \begin{cases} \dfrac{(m+1)A_p g(\theta) T_s(\theta)}{2\pi(z^2+\omega^2)} \cos^m(\phi)\cos(\theta), \\ \qquad 0 \le \theta \le \Theta_F \\ 0, \\ \qquad \theta < \Theta_F \end{cases} \tag{1}$$

with the Lambertian index $m = -1/\log_2(\cos(\theta_{1/2})$ with half-intensity radiation angle $\theta_{1/2}$; the photo-detector physical area A_p; the horizontal distance from the optical detector of the mobile user to the α^{th} LiFi AP is z; the room height is ω; the incidence and irradiation angles are θ and ϕ, respectively; the half angle of filed-of-view (FOV) of the receivers is Θ_F; the gain of the optical filter is $T_s(\theta)$; the concentrator gain $g(\theta)$ is [27]:

$$g(\theta) = \begin{cases} \dfrac{\chi^2}{\sin^2(\Theta_F)}, & 0 \le \theta \le \Theta_F \\ 0, & \theta < \Theta_F \end{cases} \tag{2}$$

where χ is the refractive index.

The reflection component may be disregarded when using LiFi with baseband modulation bandwidth (B) less than 25 MHz [26]. Furthermore, 95% or more of the total energy captured by LiFi PDs is accounted for by the direct or line-of-sight (LoS) component [28], [29]. So, given that the assumed bandwidth $B = 20$ MHz, the reflection component will be neglected in our analyzed model of the LiFi channel. Baseband communication using intensity modulation (IM) and direct detection (DD) is used in LiFi systems to transmit LiFi signals in optical power form [30]. According to [31] the average DC optical power P_{opt} and the average electric power of signals P_{elec} are converted using

$$\iota = P_{opt}/\sqrt{P_{elec}} \tag{3}$$

From [27], the signal-to-interference-plus-noise ratio (SINR) at any mobile user μ, that is allocated to α AP is:

$$\text{SINR}_{\mu,\alpha} = \frac{(\kappa P_{opt} H_{\mu,\alpha})^2}{\iota^2 N_0 B + (\kappa P_{opt})^2 \sum H_{\mu,else}^2} \tag{4}$$

where κ is the receivers' optical to electric conversion efficiency; The noise power spectral density is $N_0[A^2/Hz]$, the channel gain between the μ^{th} user and the α^{th} LiFi AP is $H_{\mu,\alpha}$, and the channel gain between the μ^{th} user and the interfering LiFi APs is $H_{\mu,else}$, according to Eq. (1). The achievable data rate between the LiFi AP α and the assigned mobile user μ is determined using the Shannon capacity as follows:

$$R_{\mu,\alpha}^{(n)} = B\log_2(1 + \text{SINR}_{\mu,\alpha}^{(n)}), \tag{5}$$

C. THE WIGIG CHANNEL MODEL

One WiGig AP, with N_{BS} antennas and N_{RF} RF chains, and N_μ mobile users, each with N_{MS} antennas, make up the postulated WiGig communication sub-network. Each mobile

user μ is considered to be connected to the WiGig AP through a single stream. Moreover, N_{max} concurrent users can be assigned to the WiGig AP [14].

For U mobile users in the downlink, the BS apply a $U \times U$ baseband precoder $F_{BB} = [f_1^{BB}, f_2^{BB}, \cdots, f_U^{BB}]$ then an $N_{BS} \times U$ RF precoder, $F_{RF} = [f_1^{RF}, f_2^{RF}, \cdots, f_U^{RF}]$ [32]. The transmitted signal could be represented as;

$$x = F_{RF} F_{BB} s, \tag{6}$$

where $s = [s_1, s_2, \cdots, s_U]^T$ is the $U \times 1$ transmitted symbols vector with $E[ss^*] = (P/U)I_U$, and average total transmitted power P.

For the sake of simplicity, the received signal at the μ^{th} user is assumed to be in the narrowband block-fading channel model used in [13], [14], [32], and [33], and could be expressed as;

$$r_\mu = H_\mu \sum_{n=1}^{U} F_{RF} f_n^{BB} s_n + n_\mu \tag{7}$$

where the $N_{MS} \times N_{BS}$ matrix; H_μ is the mmWave channel between the WiGig AP and the μ^{th} user, and the Gaussian noise that is corrupting the signal at the receiver is $n_\mu \sim N(0, \sigma^2 I)$.

The RF combiner w_μ addresses the received signal r_μ at the μ^{th} user:

$$y_\mu = w_\mu^* H_\mu \sum_{n=1}^{U} F_{RF} f_n^{BB} s_n + w_\mu^* n_\mu \tag{8}$$

To account for the anticipated limited scattering in the mmWave channel, authors in [32] utilized a geometric channel model with L_u scatterers for user u's channel. Each scatterer was thought to stand for a different propagation route from the BS to the user u. A straightforward geometric description of the scattering environment and an intermediary virtual channel representation that embodies the essence of physical modeling without its complexity were presented in [34]. The channel H_μ in this model can be stated as;

$$H_\mu = \sqrt{\frac{N_{BS} N_{MS}}{L_\mu}} \sum_{l=1}^{L_\mu} \rho_{\mu,l} a_{MS}(\theta_{\mu,l}) a_{BS}^*(\phi_{\mu,l}), \tag{9}$$

where $\rho_{\mu,l}$ is l^{th} path complex gain, with $\mathbb{E}[|\rho_{\mu,l}|^2] = \overline{\rho}$. $\theta_{\mu,l}$ and $\phi_{\mu,l} \in [0, 2\pi]$ are the l^{th} path's angles of arrival and departure (AoAs/AoDs), respectively. Finally, $a_{MS}(\theta_{\mu,l})$ and $a_{BS}^*(\phi_{\mu,l})$ are the antenna array response vectors of the AP and μ^{th} user respectively. Then, the μ's user achievable rate is represented as [32];

$$R_\mu = \log_2\left(1 + \frac{\frac{P}{U}|w_\mu^* H_\mu F_{RF} f_\mu^{BB}|^2}{\frac{P}{U}\sum_{n \neq \mu}|w_\mu^* H_\mu F_{RF} f_n^{BB}|^2 + \sigma^2}\right). \tag{10}$$

The sum-rate of the system is then:

$$R_{sum} = \sum_{\mu=1}^{N_{max}} R_\mu. \tag{11}$$

D. SEPARATE OPTIMIZATION ALGORITHM (SOA)

The SOA algorithm sequentially optimizes the APA and RA procedures [24]. To maximize the spatial SE of the LiFi network, in APA process, users whose LiFi data rates exceed a particular threshold γ will be assigned to LiFi APs. In contrast, all other users will be assigned to RF APs. The maximal effective throughput criterion is additionally used. For each user μ, assuming that:

$$r_{\mu,c} = \begin{cases} R_{\mu,\alpha}, & c \in \mathcal{C}_\mathcal{L} \quad \text{Eq. 5} \\ R_\mu, & c \in \mathcal{C}_\mathcal{R} \quad \text{Eq. 10} \end{cases} \tag{12}$$

The chosen maximal link data rate LiFi AP is [24]:

$$\tau_{1,\mu} = \arg\max_{j \in \mathcal{C}_\mathcal{L}} r_{\mu,j}, \tag{13}$$

where $r_{\mu,j}$ is the LiFi data rate. The potential data rate of each user in the attocell, assuming that all users share time resources equally, is:

$$\lambda_\mu = r_{\mu,j}/M_{\tau_{1,\mu}} \tag{14}$$

where $M_{\tau_{1,\mu}}$ is the number of users the LiFi AP $\tau_{1,\mu}$ is assigned. The following criteria will be used to allocate users with $\lambda_\mu < \gamma$ to RF APs [24]:

$$\tau_{2,\mu} = \arg\max_{j \in \mathcal{C}_\mathcal{R}} r_{\mu,j}, \qquad \lambda_\mu < \gamma. \tag{15}$$

Eqs. (13) and (15) show that in SOA, the APA outcome is:

$$g_{\mu,\alpha}^{(\text{SOA})} = \begin{cases} 1, & \alpha = \begin{cases} \tau_{1,\mu}, & \lambda_\mu \geq \gamma \\ \tau_{2,\mu}, & \lambda_\mu < \gamma \end{cases} \\ 0, & \text{Otherwise} \end{cases} \tag{16}$$

Each AP allocates the time resources to the participants individually during the RA stage. The generalized β-proportional fairness function $\Psi_\beta(x)$ may be used to express the utility maximization problem that considers both user fairness and sum-rate [35], where;

$$\Psi_\beta(x) = \begin{cases} \log(x), & \beta = 1 \\ \dfrac{x^{1-\beta}}{1-\beta}, & \beta \geq 0, \beta \neq 1 \end{cases} \tag{17}$$

where x is the achievable data rate and β is the fairness coefficient. The RA stage can be described as follows:

$$k_{\mu,\alpha}^{(\text{SOA})} = \frac{r_{\mu,\alpha}^{\frac{1}{\beta}-1}}{\sum_{i \in \mathcal{U}_\alpha} r_{i,\alpha}^{\frac{1}{\beta}-1}} \quad (\beta > 0). \tag{18}$$

The SOA stages are summarized in Algorithm 1.

The selected threshold γ will significantly impact the SOA algorithm's performance. The number of users assigned to a specific LiFi AP $M_{\tau_{1,\mu}}$ may be rather large due to the random distribution of the mobile users. The potential data rate λ_μ in Eq. (14) will be under the accepted level due to the LiFi APs' resource limitations. If γ is somewhat more than the threshold, with high probability, λ_μ will be smaller than γ. As a result, the WiGig AP will be allocated to all of these

Algorithm 1 SOA Algorithm

Initialisation: $r_{\mu,\alpha}$ and γ;
for *each user* μ_i; $i = 1$ *to* N_μ **do**
  Using Eqs.(13, 14), the CPU determines $\tau_{1,\mu}$ and the optical data rate λ_μ, respectively
end for
if $\lambda_\mu \geq \gamma$ **then**
  Assign the user to the LiFi AP $\tau_{1,\mu}$;
else
  Assign the user to the RF AP $\tau_{2,\mu}$ using Eq. (15);
end if
According to Eq. (18), each AP decides the resource fraction for its assigned users in the RA stage.

Algorithm 2 CAWFS Algorithm

Initialisation: $r_{\mu,\alpha}$, N_{max}, all users are considered as LiFi users in the $\mathcal{M}$ set, and count = 0;
while *count* $< N_{max}$ **do**
  $\tau_{1,\mu}$ and λ_μ are calculated;
  The user having the minimum data rate, μ_{min}, is assigned to WiGig AP;
  Update; $\mathcal{M} = \mathcal{M} - \mu_{min}$, count = count + 1;
end while
Using Eq. (18) in the RA stage, each AP decides the resource fraction for its assigned users.

users, leaving the LiFi AP idle and underutilizing network resources. As another example of resource underutilization, if the threshold γ is set to an extremely low value, no users or just a minimal number of users will be allocated to the WiGig AP. This problem is solved in the CAWFS algorithm II-E.

E. CONSECUTIVE ASSIGN WIGIG FIRST SOA (CAWFS) LB ALGORITHM

The CAWFS method sequentially assigns each one of the N_{max} users to a WiGig AP, one at a time [17]. All users are initially grouped into a set $\mathcal{M}$, and using Eq. (13), each user is assigned to LiFi AP. The user with the lowest possible LiFi rate μ_{min}, Eq. (14), is assigned to the WiGig AP and deleted from $\mathcal{M}$. Using Eq. (13), the remaining users in $\mathcal{M} = \mathcal{M} - \mu_{min}$ are then divided up among the LiFi APs, and the new potential γ_μ is then calculated. The above-mentioned step is repeated until N_{max} users, the allowed maximum, are allocated to the WiGig AP. The APA output of the CAWFS algorithm may be shown as follows [17]:

$$g_{\mu,\alpha}^{(\mathrm{CAWFS})} = \begin{cases} 1, & \alpha = \begin{cases} \tau_{1,\mu}, & \mu \in \mathcal{M} \\ \text{WiGig AP}, & \mu \notin \mathcal{M} \end{cases} \\ 0, & \text{Otherwise} \end{cases} \tag{19}$$

III. PROPOSED MCD LOAD BALANCING ALGORITHM

This article proposes an indoor WLAN hybrid network combining LiFi and WiGig technologies. In a hybrid network, only one, LiFi or WiGig, AP can provide service to each user for downlink communications; hence LB should be considered. In earlier LB systems, it was proposed to repeatedly run complex optimization APA algorithms with each iteration ending within quasi-static state T_n, where n denotes the sequence number of the stages [26]. In order to offer a proper performance/complexity trade-off, the MCD algorithm is proposed in this paper. The MCD technique can generate significant system throughput and significantly reduce computational complexity. The key strategy of the proposed algorithm is to not repeat the APA calculations for each users' distributions. The MCD algorithm aims to utilize the history of all possible mobile users' distributions and their corresponding APA decisions recorded in a Distributions-Decisions Record (DDR) to select the most suitable decisions for the new mobile users' distribution. The proposed MCD scheme composes of two stages:

1) **Distributions-Decisions Record Construction Stage.** The Distributions-Decisions Record (DDR) is a list (lookup table) of the most used case users' distributions (mobile users' fingerprints) in the covered area and their corresponding best APA decisions for each distribution, which are calculated depending on the CAWFS algorithm [17]. The DDR is constructed once offline by the CPU. Each raw in the DDR comprises the supposed distribution from the distribution matrix DM and the corresponding decisions. The decision of each user is:

$$D_u \in \{D_i\}_{(i=0)}^{(N_{LF})} \tag{20}$$

where $i = 0$ is used for WiGig AP, and others are used for LiFi APs. The pseudo algorithm for the DDR construction process is shown in Algorithm 3.

Algorithm 3 DDR Construction Algorithm
This algorithm is running once and offline by the CPU

Initialisation: $r_{\mu,\alpha}$, N_{max}, size of DDR $\mathcal{S}$, DM matrix, initial $\mathcal{DDR} = \phi$ and count = 0 ;
while *count* $< \mathcal{S}$ **do**
  Calculate the decision vector $\mathcal{D}$ for the c^{th} raw of the DM matrix $DM(c)$ using CAWFS algorithm (2);
  Update the DDR; $\mathcal{DDR} = [\mathcal{DDR}; [DM(c) \ \ \mathcal{D}]]$, count = count + 1;
end while
Output: $\mathcal{DDR}$;

2) **Decisions Selection (DS) Stage.** Given the current distribution of mobile users in $1 \times 2N_u$ vector d_u, the current decisions are chosen depending on the modified majority voting technique as follows:

i The second order statistics (SOS), i.e., the correlation between the current distribution and all recorded distributions in the DDR are calculated to form the correlation $\mathcal{S} \times 1$ vector $\mathcal{C}_{\mathcal{D}}$.

ii The indices of the correlation values above a certain threshold c_{th} in $\mathcal{C}_{\mathcal{D}}$ are chosen, and the corresponding decisions are selected to form the voting matrix $\mathcal{V}_{\mathcal{T}}$.

iii The majority voting for each column in $\mathcal{V}_{\mathcal{T}}$ is calculated, as explained in III-A, where;

$$[D_u(n), m(n)] = MV[\mathcal{V}_{\mathcal{T}}(n)] \quad \text{for } n = 1 \text{ to } N_u; \tag{21}$$

where $MV[X]$ is the majority voting for the vector X, $D_u(n)$ and $m(n)$ are the decision with majority voting and the number of votes for it in the column n, respectively.

iv Only N_{max} users, with highest number of votes m as $D_u = D_0$, will be allocated to WiGig AP.

v The updated voting matrix for LiFi APs $\mathcal{V}_{\mathcal{LF}}$ is constructed by elimination the indices of all WiGig AP users in $WiGig_u$ vector from $\mathcal{V}_{\mathcal{T}}$.

$$\mathcal{V}_{\mathcal{LF}} = \mathcal{V}_{\mathcal{T}} - \mathcal{V}_{\mathcal{T}}[:, WiGig_u]; \tag{22}$$

vi The LiFi APs users are allocated depending on the majority voting of each column of the updating voting matrix $\mathcal{V}_{\mathcal{LF}}$.

$$[D_u(n), m(n)] = MV[\mathcal{V}_{\mathcal{LF}}(n)] \quad \text{for } n = 1 \text{ to } N_u - N_{max}; \tag{23}$$

The pseudo algorithm for the DS stage is shown in Algorithm 4.

Algorithm 4 DS Algorithm

Initialisation: $\mathcal{DDR}$, d_u, and count $= 0$;
DM is a part of the $\mathcal{DDR}$ where;
$DM = \mathcal{DDR}(:, 1 : 2N_u)$;
$\mathcal{C}_{\mathcal{D}} = Corr(d_u, DM)$;
Construction of the voting matrix:
while $count < \mathcal{S}$ **do**
  if $\mathcal{C}_{\mathcal{D}}(count) \geq c_{th}$ **then**
    Update the indices vector $\mathcal{V}_{\mathcal{T}}$ where;
    $\mathcal{V}_{\mathcal{T}} = [\mathcal{V}_{\mathcal{T}};\ \mathcal{DDR}(count, 2N_u : end)]$
  end if
end while
Assignment of the WiGig AP users:
for $n = 1$ *to* N_u **do**
  $[D_u(n), m(n)] = MV[\mathcal{V}_{\mathcal{T}}(n)]$
end for
end for
$WiGig_u = find(N_{max} - Largest(m) | D_u = D_0)$
Construction of the LiFi users voting matrix:
$\mathcal{V}_{\mathcal{LF}} = \mathcal{V}_{\mathcal{T}} - \mathcal{V}_{\mathcal{T}}[:, WiGig_u]$;
Assignment of the LiFi AP users:
for $n = 1$ *to* $N_u - N_{max}$ **do**
end for
$[D_u(n), m(n)] = MV[\mathcal{V}_{\mathcal{LF}}(n)]$
end for
Output: $D_u \in \{D_i\}_{(i=0)}^{(N_{LF})}$ where; $i = 0$ for WiGig AP, and others for LiFi APs;

A. MAJORITY VOTING SELECTION

Given the voting matrix $\mathcal{V}_{\mathcal{T}}$, each column's majority voting decision has the highest repeating probability. An example of the majority voting selection method is shown in Table 1 where five groups of Suggested Decisions (SDs) for different highly correlated distributions of 5 Mobile Users (MUs) are given, and the Majority Voting Decision (MVD) are calculated.

TABLE 1. Example of majority voting algorithm.

-	MU1	MU2	MU3	MU4	MU5
SDs 1	D0	D1	D2	D0	D4
SDs 2	D0	D2	D2	D4	D4
SDs 3	D1	D2	D2	D1	D3
SDs 4	D0	D2	D2	D4	D3
SDs 5	D0	D1	D1	D4	D3
MVD	**D0**	**D2**	**D2**	**D4**	**D3**

B. COMPUTATION COMPLEXITY ANALYSIS

The proposed LB scheme's computational complexity (CC) is analyzed in terms of the number of multiplication operations (MO) [24] and compared with the CC of CAWFS and SOA schemes. The SOA number of MO is off order $\sim O(N_u)$ [1] and the MO in the CAWFS is of order $O(AP\sum_{i}^{N_{max}}(N_u - i))$, where AP is the total number of WiGig and LiFi APs [17], while the proposed MCD is of order $\sim O(2N_u)$ since it is only depending on the correlation vector. It is clear that the CC order of the proposed MCD is twice the SOA while it is much lower than the CC order of CAWFS. In CC analysis of CAWFS and SOA, the MO for Eq. (13) to Eq. (15) are not considered as they are fixed and repeated for each UE and over each iteration.

IV. PERFORMANCE EVALUATION

A. SIMULATION SETUP

The identical system configuration and simulation settings from [19], [23], [26], [36], and [17] are applied in this simulation part. We consider a hybrid network with one WiGig AP and four LiFi APs. It has been demonstrated with WiGig AP that the throughput advantage decreases as N_{max} increases [12], [13]. In this work, and depending on simulation results in [17] and in subsection IV-C, N_{max} is chosen to be 6 users. Under the assumption that there is no optical ICI, every LiFi attocell in a circle with a radius of 4 meters uses the same frequency band. The covered indoor space has a 16×16 m^2 area. Each pair of adjacent LiFi APs is located 8 meters apart. Using the random way-point paradigm, users are randomly distributed and randomly move [37], [38]. According to this model, each node moves at a

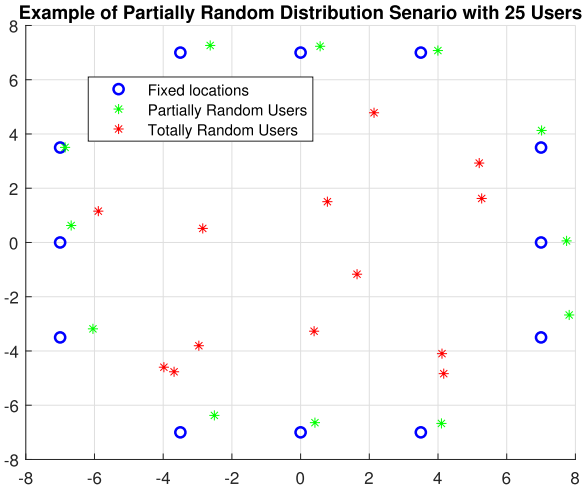

FIGURE 2. Example of partially random users' distribution.

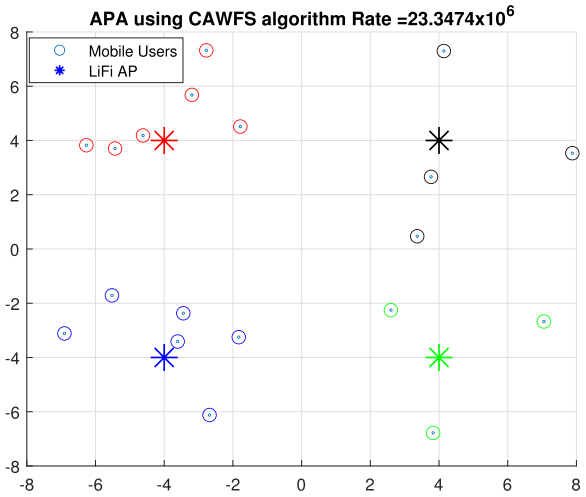

FIGURE 3. Example of APA using CAWFS algorithm.

TABLE 2. Parameters of simulation.

Name of Parameters	Value
The parameters of LiFi APs	
The radius of LiFi attocell	4 m
The height of the covered room	2.3 m
Converting electrical energy into optical energy, ι	1
The transmitted optical power of the LiFi AP, Pt	10 W
LED light baseband bandwidth, B	20 MHz
The physical area of the photo detector PD, A_p	1 cm^2
Half-intensity radiation angle, $\theta_{1/2}$	60 deg
The optical filter gain, $T_s(\theta)$	1.0
FoV semi-angle of the receiver, Θ_F	60 deg
Refractive index, χ	1.5
Efficiency of optical to electric conversion, κ	0.53 A/W
Noise power spectral density, N_0	$10^{-19} A^2/Hz$
The time frame for resource distribution, T_p	500 ms
The parameters of the WiGig APs	
Number of antennas in the base station side, N_{BS}	25
Number of antennas in the mobile user side, N_{MS}	9
Maximum number of the WiGig AP users, N_{max}	6
Channel SNR,	0 dB
Number of paths, l	1

speed that is uniformly dispersed across the interval [$V_{min} = 0.3\ m/sec$, $V_{max} = 0.7\ m/sec$] to a chosen target site. Once the target has been attained, the node pauses for a certain period of time before choosing a new target to move toward at a different speed. The available area is basically covered by a partially random distribution (PRD) scenario. In the PRD, some users are partially tied, within 0.5 m distance, to certain fixed locations to simulate users set around offices or fixed tables, and the rest of the users are free to move to any point in the coverage area. Examples of PRD distributions are shown in Fig. 2. Table 2 provides a summary of the other parameters.

Based on the achievable data rates and outage probability measurements, the proposed MCD, SOA and the CAWFS algorithms are compared for downlink communications. For all algorithms, the user data rate in state n is computed as follows:

$$R_{\mu}^{(n)} = \frac{1}{N_{\mu}} \sum_{\alpha \in \mathcal{C}} g_{\mu,\alpha}^{(n)} k_{\mu,\alpha}^{(n)} r_{\mu,\alpha}^{(n)}, \tag{24}$$

where $g_{\mu,\alpha}^{(n)}$ is given in Eq. (16), and Eq. (19) for SOA, and CAWFS algorithm, respectively.

In this section, one example for APA of both MCD and CAWFS algorithms, in PRD scenario, will be shown. Then, the effect of N_{max} variation on the WiGig sub-network performances such as achievable data rate and outage probability will be tested to determine its suitable value for the supposed system setup. The effect of the most important parameters, the correlation threshold, on the achievable data rate and outage probability will be examined. Then, we will examine the visibility of applying the proposed MCD algorithm with various numbers of mobile users. After this, the effect of the chosen size of the DDR record on the achievable data rate and outage probability will be tested. In the end, some of the previous simulation results are recalculated in another user distribution model; fully random distribution (FRD).

B. EXAMPLE OF APA USING DIFFERENT ALGORITHMS

In this part, two examples of APA of both MCD and CAWFS algorithms are shown in Fig. 4, with an average LiFi bit rate of 22.2 Mbps and Fig. 3 with an average LiFi bit rate of 23.3 Mbps, respectively. Given that $N_{max} = 6$, $N_{\mu} = 25$ mobile users are distributed between one WiGig AP and 4 LiFi APs in this experiment. The access points and their assigned users have the same colors. It is shown that MCD and CAWFS allocation algorithms have almost the same mobile users distributions with a little bit smaller achievable average data rate in MCD algorithm.

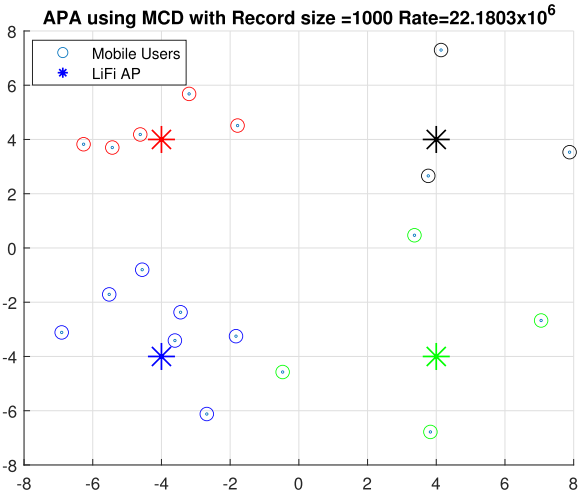

FIGURE 4. Example of APA using MCD algorithm.

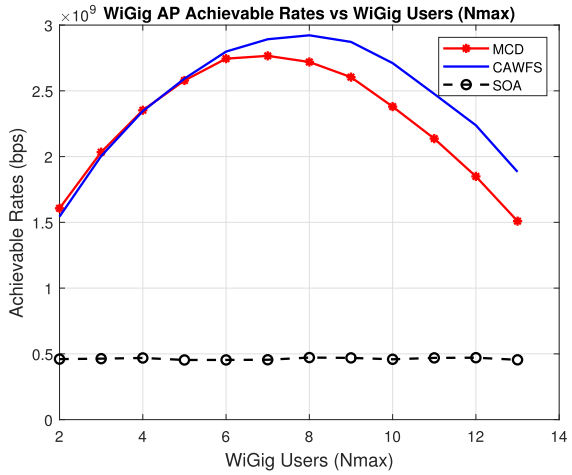

FIGURE 5. Achievable rates vs number of users of WiGig AP at $\Gamma = 30$ Mbps.

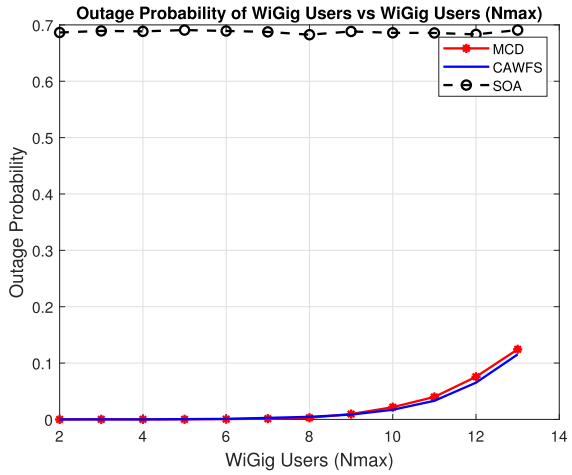

FIGURE 6. Outage probability vs number of users of WiGig AP at $\Gamma = 30$ Mbps.

C. THE OPTIMAL NUMBER OF WIGIG AP USERS

It has been demonstrated with WiGig AP that the throughput advantage decreases as N_{max} increases [12], [13]. This part

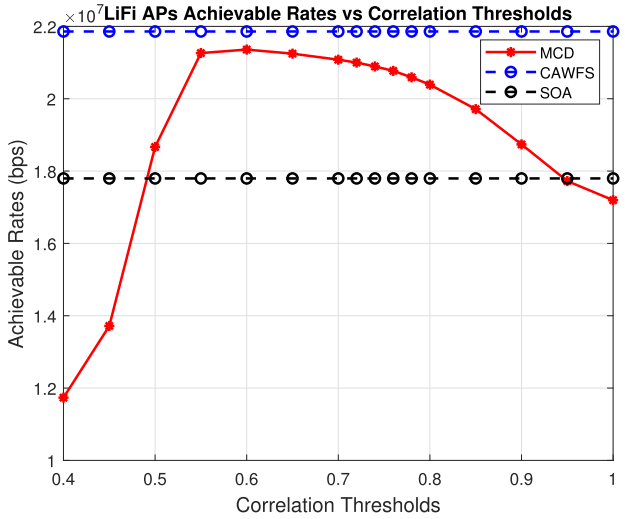

FIGURE 7. Achievable data rates vs correlation thresholds $\mathcal{C}_{\mathcal{V}}$ for partially random users' distribution.

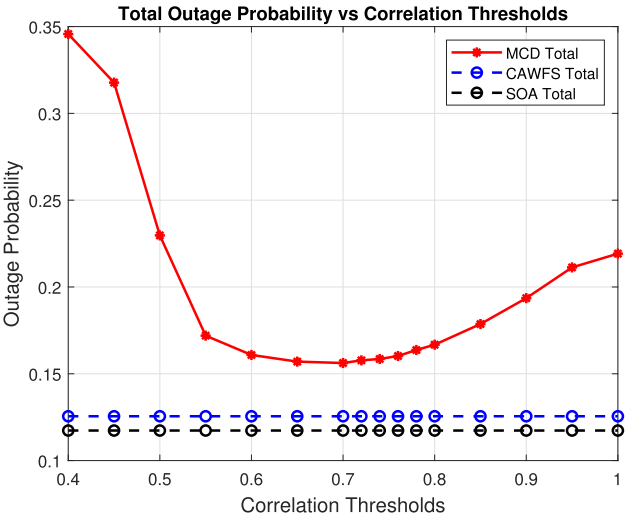

FIGURE 8. Total outage probability calculations vs correlation thresholds $\mathcal{C}_{\mathcal{V}}$ for partially random users' distribution.

tests the effect of N_{max} variation on the WiGig sub-network results such as achievable data rate and outage probability. For each user, the outage probability is defined as:

$$\Phi_0 = \Pr(R_{\mu}^{n} < \Gamma_0), \tag{25}$$

where Γ_0 is a uniform minimum data rate offered to users. Using Monte Carlo simulations, the outage probability is calculated as follows:

$$\Phi_0 = \frac{\Sigma_n \text{Number of Users with} R_{\mu}^{n} < \Gamma_0}{\Sigma_n \text{Number of Total Users}} \tag{26}$$

In Fig. 5, the simulation results of achievable rates for WiGig AP users, show that the maximum number of users could be assigned to WiGig AP N_{max} could be in the range of 6-to-8 users, which agree with the simulation results in [14]. In Fig. 6, given that $\Gamma = 30$ Mbps, the outage probability is less than 1% in the above-mentioned rang.

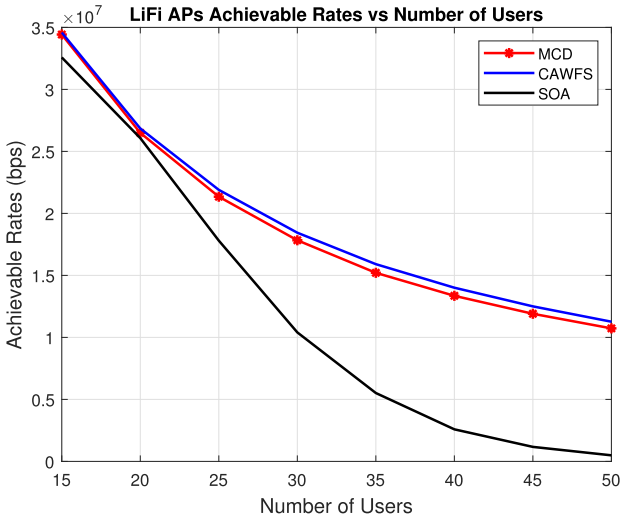

FIGURE 9. LiFi achievable data rates vs number of users for partially random users' distribution.

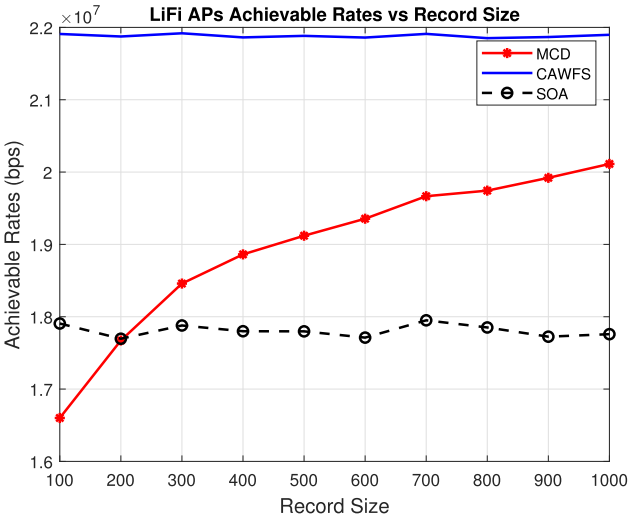

FIGURE 11. LiFi achievable data rates vs distributions-decisions record (DDR) size for partially random users' distribution.

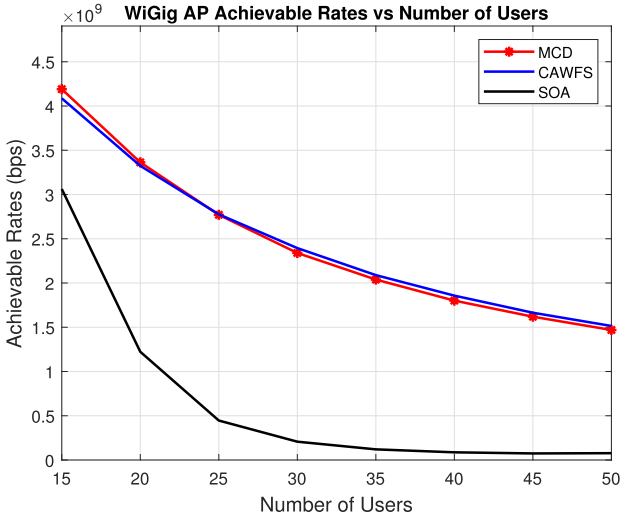

FIGURE 10. WiGig achievable data rates vs number of users for partially random users' distribution.

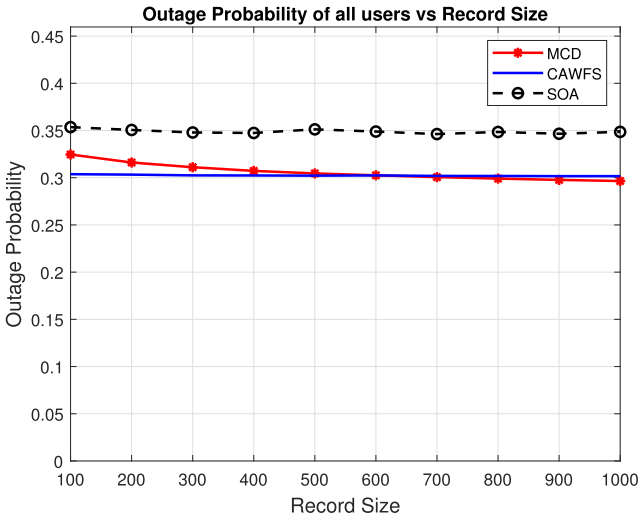

FIGURE 12. Average outage probability vs distributions-decisions record (DDR) size for partially random users' distribution.

D. THE ACHIEVABLE DATA RATE VS CORRELATION THRESHOLD $\mathcal{C}_\mathcal{V}$

This part examines the effect of the chosen value of the correlation threshold $\mathcal{C}_\mathcal{V}$. Figs. 7 shows the average achievable data rate for LiFi APs using all algorithms as a function of correlation threshold $\mathcal{C}_\mathcal{V}$ in PRD distribution scheme. The simulation results show that the MCD algorithm's performance could be accepted compared to the CAWFS algorithm if the suitable correlation threshold $\mathcal{C}_\mathcal{V}$ is chosen. In this context, the MCD algorithm achieves performance better than the performance of the SOA reference algorithm.

E. THE OUTAGE PROBABILITY VS CORRELATION THRESHOLD $\mathcal{C}_\mathcal{V}$

A uniform minimum data rate offered to users, Γ_0, is considered when calculating the outage probability. Fig. 8 shows the outage probability as a function of correlation threshold $\mathcal{C}_\mathcal{V}$ in the PRD distribution scheme. The simulation results show that the MCD algorithm could achieve an accepted outage probability compared to the CAWFS algorithm if the suitable correlation threshold $\mathcal{C}_\mathcal{V}$ is chosen.

F. THE IMPACT OF ALTERING THE OVERALL NUMBER OF MOBILE USERS N_μ

This subsection examines the visibility of applying the proposed MCD algorithm with various numbers of mobile users. For LiFi and WiGig users, the achievable data rates are calculated as functions of the total number of users N_μ in Figs 9 and 10 in PDR distribution scenario. The results demonstrated that the proposed MCD algorithm performs nearly as well as the CAWFS algorithm. Moreover,

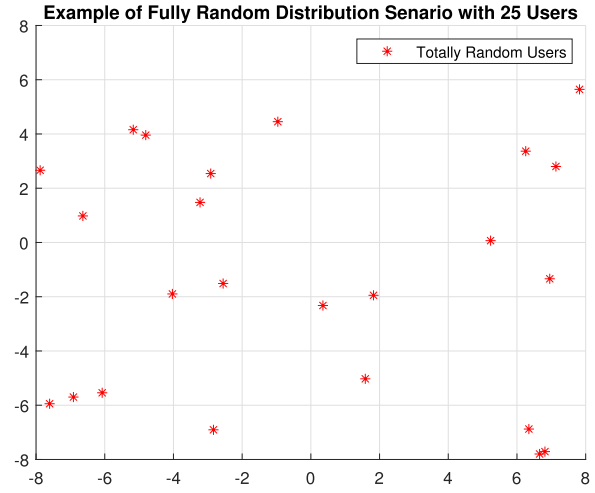

FIGURE 13. Example of fully random users' distribution.

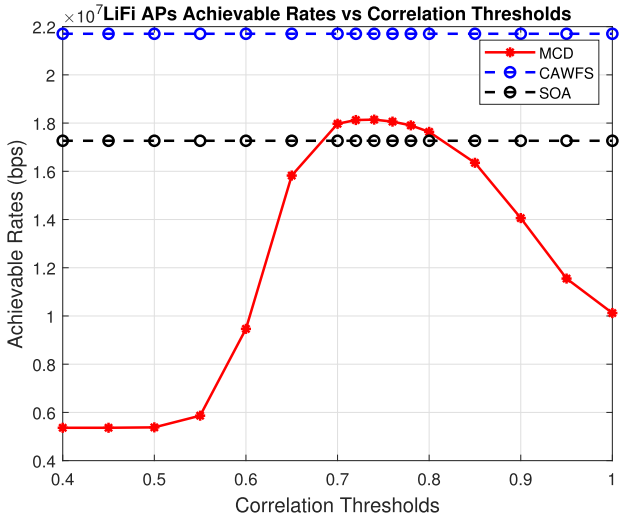

FIGURE 14. Achievable data rates vs correlation thresholds $\mathcal{C}_{\mathcal{V}}$ for fully random users' distribution.

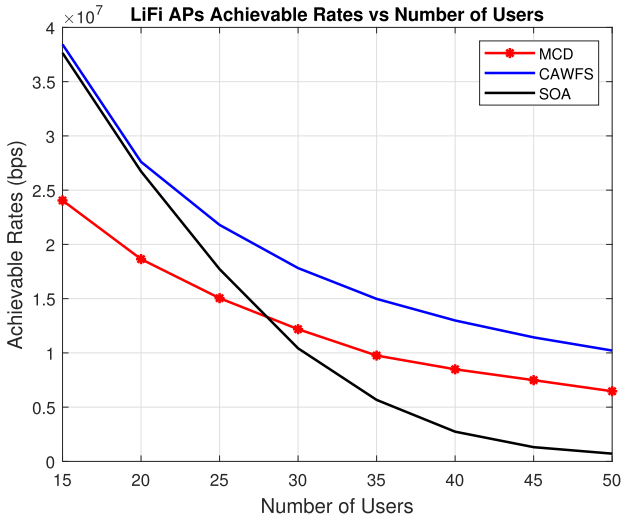

FIGURE 15. LiFi achievable data rates vs number of users for fully random users' distribution.

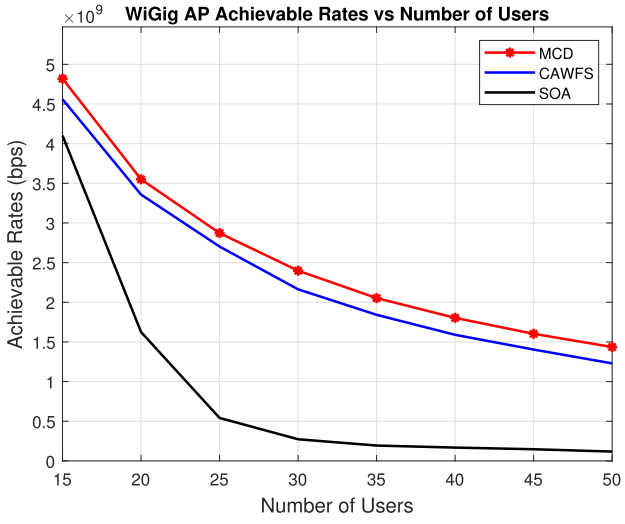

FIGURE 16. WiGig achievable data rates vs number of users for fully random users' distribution.

both algorithms outperform the performance when using SOA.

G. DECISION-DISTRIBUTION RECORD (DDR) SIZE EFFECT

This subsection examines the effect of the available DDR size on the achievable data rate and outage probability. In Figs. 11 and 12 for the PDR distribution scenario, the simulation results for the achievable data rates and average outage probability of LiFi APs as functions of DDR size are presented. The results demonstrated that the proposed MCD algorithm's performance converges with the CAWFS algorithm's. Moreover, both algorithms perform better than SOA algorithm.

H. FULLY RANDOM DISTRIBUTION (FRD) SCENARIO

In this part, some of the previous simulation results are recalculated in another user distribution model; fully random distribution (FRD). In the FRD all users can move to any point in the coverage area. Example of the FRD distribution is shown in Fig. 13.

Fig. 14 shows the average achievable data rate for LiFi APs using all algorithms as a function of correlation threshold $\mathcal{C}_{\mathcal{V}}$ in FRD distribution schemes. The simulation results show that the MCD algorithm's performance could be accepted compared to the CAWFS algorithm if the suitable correlation threshold $\mathcal{C}_{\mathcal{V}}$ is chosen. In this context, the MCD algorithm achieves performance better than the performance of the SOA reference algorithm.

For LiFi and WiGig users, the achievable data rates are calculated as functions of the total number of users N_{μ} in Figs 15 and 16 in FDR distribution scenario. The results demonstrated that the proposed MCD algorithm performs nearly as well as the CAWFS algorithm. Moreover, both algorithms outperform the performance when using SOA.

V. CONCLUSION

This paper proposes the most-correlated distribution (MCD) based load balancing strategy. The major goal of the suggested MCD method is to prevent having to repeatedly run the APA optimization computations for each user's distribution. Instead, considering the history of all possible distributions of mobile users and their related APA decisions, which are recorded in the Distributions-Decisions Record (DDR), the MCD algorithm has enough intelligence to find the optimum decisions for the current distribution of mobile users. The central processing unit (CPU) creates the DDR record once, off-line, using the CAWFS method. The subset of the DDR records that has the most correlated distributions is selected depending on the new mobile user distribution. The majority voting method is used to pick the new decisions based on the prior decisions made in the specified subset. The proposed approach provides performance characteristics, for feasible data rate throughput and outage probability, that are comparable to those of the most recent load-balancing algorithms while needing less complexity.

REFERENCES

[1] D. Tsonev, H. Chun, S. Rajbhandari, J. J. McKendry, S. Videv, E. Gu, M. Haji, S. Watson, A. E. Kelly, G. Faulkner, M. D. Dawson, H. Haas, and D. O'Brien, "A 3-Gb/s single-LED OFDM-based wireless VLC link using a gallium nitride μLED," *IEEE Photon. Technol. Lett.*, vol. 26, no. 7, pp. 637–640, Jan. 2014.

[2] H. S. Hussein and M. Hagag, "Optical MIMO-OFDM with fully generalized index-spatial LED modulation," *IEEE Commun. Lett.*, vol. 23, no. 9, pp. 1556–1559, Sep. 2019.

[3] H. S. Hussein, "Optical polar based MIMO-OFDM with fully generalised index-spatial LED modulation," *IET Commun.*, vol. 14, no. 2, pp. 282–289, Jan. 2020.

[4] H. S. Hussein, M. Hagag, and M. Farrag, "Extended spatial-index LED modulation for optical MIMO-OFDM wireless communication," *Electronics*, vol. 9, no. 1, p. 168, Jan. 2020.

[5] R. Sharma, D. S. Gurjar, E. Rahman, A. Raghav, P. Shukla, and V. Mishra, "LiFi technology: A breakthrough for massive data rates in indoor applications," in *Intelligent Systems for Social Good: Theory and Practice*. Singapore: Springer, 2022, pp. 63–79.

[6] M. R. Ghaderi, "LiFi and hybrid WiFi/LiFi indoor networking: From theory to practice," *Opt. Switching Netw.*, vol. 47, Feb. 2023, Art. no. 100699.

[7] H. Haas, L. Yin, C. Chen, S. Videv, D. Parol, E. Poves, H. Alshaer, and M. S. Islim, "Introduction to indoor networking concepts and challenges in LiFi," *J. Opt. Commun. Netw.*, vol. 12, no. 2, pp. A190–A203, Feb. 2020.

[8] D. A. Basnayaka and H. Haas, "Hybrid RF and VLC systems: Improving user data rate performance of VLC systems," in *Proc. IEEE 81st Veh. Technol. Conf. (VTC Spring)*, May 2015, pp. 1–5.

[9] S. Shao, A. Khreishah, M. B. Rahaim, H. Elgala, M. Ayyash, T. D. Little, and J. Wu, "An indoor hybrid WiFi-VLC internet access system," in *Proc. IEEE 11th Int. Conf. Mobile Ad Hoc Sensor Syst.*, Oct. 2014, pp. 569–574.

[10] M. B. Rahaim, A. M. Vegni, and T. D. C. Little, "A hybrid radio frequency and broadcast visible light communication system," in *Proc. IEEE GLOBECOM Workshops (GC Wkshps)*, Dec. 2011, pp. 792–796.

[11] Z. Pi and F. Khan, "An introduction to millimeter-wave mobile broadband systems," *IEEE Commun. Mag.*, vol. 49, no. 6, pp. 101–107, Jun. 2011.

[12] W. Wu, Q. Shen, M. Wang, and X. Shen, "Performance analysis of IEEE 802.11.ad downlink hybrid beamforming," in *Proc. IEEE Int. Conf. Commun. (ICC)*, May 2017, pp. 1–6.

[13] I. Ahmed, H. Khammari, and A. Shahid, "Resource allocation for transmit hybrid beamforming in decoupled millimeter wave multiuser-MIMO downlink," *IEEE Access*, vol. 5, pp. 170–182, 2017.

[14] G. Kwon, Y. Shim, H. Park, and H. M. Kwon, "Design of millimeter wave hybrid beamforming systems," in *Proc. IEEE 80th Veh. Technol. Conf. (VTC-Fall)*, Sep. 2014, pp. 1–5.

[15] T. Besjedica, K. Fertalj, V. Lipovac, and I. Zakarija, "Evolution of hybrid LiFi–WiFi networks: A survey," *Sensors*, vol. 23, no. 9, p. 4252, Apr. 2023.

[16] I. Lau, S. Ekpo, M. Zafar, M. Ijaz, and A. Gibson, "Hybrid mmWave-Li-Fi 5G architecture for reconfigurable variable latency and data rate communications," *IEEE Access*, vol. 11, pp. 42850–42861, 2023.

[17] M. Farrag, M. Z. Shamim, M. Usman, and H. S. Hussein, "Load balancing scheme in hybrid WiGig/LiFi network," *IEEE Access*, vol. 8, pp. 222429–222438, 2020.

[18] A. Pärssinen, M.-S. Alouini, M. Berg, T. Kürner, P. Kyösti, M. E. Leinonen, M. Matinmikko-Blue, E. McCune, U. Pfeiffer, and P. Wambacq, "White paper on RF enabling 6G: Opportunities and challenges from technology to spectrum," 6G Flagship, Univ. Oulu, Finland, Tech. Rep. 13, Apr. 2021.

[19] Y. Wang, D. A. Basnayaka, X. Wu, and H. Haas, "Optimization of load balancing in hybrid LiFi/RF networks," *IEEE Trans. Commun.*, vol. 65, no. 4, pp. 1708–1720, Apr. 2017.

[20] M. Obeed, A. M. Salhab, and S. A. Zummo, "Joint optimization for power allocation and load balancing for hybrid VLC/RF networks," U.S. Patent 16 163 750, Apr. 23, 2020.

[21] M. Obeed, A. M. Salhab, S. A. Zummo, and M.-S. Alouini, "Joint optimization of power allocation and load balancing for hybrid VLC/RF networks," *J. Opt. Commun. Netw.*, vol. 10, no. 5, pp. 553–562, May 2018.

[22] R. Badeel, S. K. Subramaniam, A. Muhammed, and Z. M. Hanapi, "A multicriteria decision-making framework for access point selection in hybrid LiFi/WiFi networks using integrated AHP–VIKOR technique," *Sensors*, vol. 23, no. 3, p. 1312, Jan. 2023.

[23] Y. Wang, X. Wu, and H. Haas, "Fuzzy logic based dynamic handover scheme for indoor Li-Fi and RF hybrid network," in *Proc. IEEE Int. Conf. Commun. (ICC)*, May 2016, pp. 1–6.

[24] Y. Wang and H. Haas, "A comparison of load balancing techniques for hybrid LiFi/RF networks," in *Proc. 4th ACM Workshop Visible Light Commun. Syst.*, Oct. 2017, pp. 43–47.

[25] I. Stefan, H. Burchardt, and H. Haas, "Area spectral efficiency performance comparison between VLC and RF femtocell networks," in *Proc. IEEE Int. Conf. Commun. (ICC)*, Jun. 2013, pp. 3825–3829.

[26] Y. Wang and H. Haas, "Dynamic load balancing with handover in hybrid Li-Fi and Wi-Fi networks," *J. Lightw. Technol.*, vol. 33, no. 22, pp. 4671–4682, Nov. 15, 2015.

[27] J. M. Kahn and J. R. Barry, "Wireless infrared communications," *Proc. IEEE*, vol. 85, no. 2, pp. 265–298, Feb. 1997.

[28] M. Hammouda, S. Akln, A. M. Vegni, H. Haas, and J. Peissig, "Hybrid RF/LC systems under QoS constraints," in *Proc. 25th Int. Conf. Telecommun. (ICT)*, Jun. 2018, pp. 312–318.

[29] T. Komine and M. Nakagawa, "Fundamental analysis for visible-light communication system using LED lights," *IEEE Trans. Consum. Electron.*, vol. 50, no. 1, pp. 100–107, Feb. 2004.

[30] C. Chen, S. Videv, D. Tsonev, and H. Haas, "Fractional frequency reuse in DCO-OFDM-based optical attocell networks," *J. Lightw. Technol.*, vol. 33, no. 19, pp. 3986–4000, Oct. 1, 2015.

[31] S. Dimitrov and H. Haas, *Principles of LED Light Communications: Towards Networked Li-Fi*. Cambridge, U.K.: Cambridge Univ. Press, 2015.

[32] A. Alkhateeb, G. Leus, and R. W. Heath Jr., "Limited feedback hybrid precoding for multi-user millimeter wave systems," *IEEE Trans. Wireless Commun.*, vol. 14, no. 11, pp. 6481–6494, Nov. 2015.

[33] O. E. Ayach, S. Rajagopal, S. Abu-Surra, Z. Pi, and R. W. Heath Jr., "Spatially sparse precoding in millimeter wave MIMO systems," *IEEE Trans. Wireless Commun.*, vol. 13, no. 3, pp. 1499–1513, Mar. 2014.

[34] A. M. Sayeed, "Deconstructing multiantenna fading channels," *IEEE Trans. Signal Process.*, vol. 50, no. 10, pp. 2563–2579, Oct. 2002.

[35] J. Mo and J. Walrand, "Fair end-to-end window-based congestion control," *IEEE/ACM Trans. Netw.*, vol. 8, no. 5, pp. 556–567, Oct. 2000.

[36] X. Wu, M. Safari, and H. Haas, "Three-state fuzzy logic method on resource allocation for small cell networks," in *Proc. IEEE 26th Annu. Int. Symp. Pers., Indoor, Mobile Radio Commun. (PIMRC)*, Aug. 2015, pp. 1168–1172.

[37] C.-L. Tsao, Y.-T. Wu, W. Liao, and J.-C. Kuo, "Link duration of the random way point model in mobile ad hoc networks," in *Proc. IEEE Wireless Commun. Netw. Conf. (WCNC)*, vol. 1, Apr. 2006, pp. 367–371.

[38] D. B. Johnson and D. A. Maltz, "Dynamic source routing in ad hoc wireless networks," in *Mobile Computing*. Boston, MA, USA: Springer, 1996, pp. 153–181.

MOHAMMED FARRAG (Member, IEEE) received the B.Sc. degree in electrical engineering and the M.Sc. degree in communication and electronics from Assiut University, Egypt, in 2001 and 2008, respectively, and the Ph.D. degree in communication and electronics engineering from the Egypt-Japan University of Science and Technology (E-JUST), in 2013. In 2012, he was a Special Researcher Student with Kyushu University, Japan. He has been an Associate Professor with the Faculty of Engineering, Assiut University, since 2019. He is currently an Assistant Professor with the College of Engineering, King Khalid University, Saudi Arabia. His research interests include digital signal processing for communications, image denoising, low-power wireless communications, cognitive radio, compressive sensing, Li-Fi technology, and visible light communication. He is a technical committee member of many international conferences and a reviewer of many international conferences, journals, and transactions.

HANY S. HUSSEIN (Senior Member, IEEE) received the B.Sc. degree in electrical engineering and the M.Sc. degree in communication and electronics from South Valley University, Egypt, in 2004 and 2009, respectively, and the Ph.D. degree in communication and electronics engineering from the Egypt-Japan University of Science and Technology (E-JUST), in 2013. In 2012, he was a Special Researcher Student with Kyushu University, Japan. He has been an Associate Professor with the Faculty of Engineering, Aswan University, since 2019. He is currently an Assistant Professor with the College of Engineering, King Khalid University, Saudi Arabia. His research interests include digital signal processing for communications, multimedia, image, and video coding, low-power wireless communications, one-bit ADC multiple-input multiple-output, underwater communication, index and spatial modulation, Li-Fi technology, and visible light communication. He is a technical committee member of many international conferences and a reviewer of many international conferences, journals, and transactions. Moreover, he was the General Co-Chair of the IEEE ITCE, in 2018.